

High- p_{\perp} charged particle azimuthal correlations at RHIC

Jan Rak¹ for the PHENIX collaboration
Iowa State University

The analysis of two-particle azimuthal correlation function in $p+p$ and $Au+Au$ collisions at $\sqrt{s_{NN}}=200$ GeV is presented. The mean jet fragmentation transverse momentum $\sqrt{\langle j_{\perp}^2 \rangle}$ and mean parton transverse momentum $\sqrt{\langle k_{\perp}^2 \rangle}$ are inferred from $p+p$ collisions. The analysis of $Au+Au$ data, where elliptic flow is a dominant source of two-particles correlation is also presented. We derive the upper limit on partonic azimuthal anisotropy based on jet-quenching in a Glauber model. We show that some new mechanism, generating the azimuthal anisotropy observed in final state, is needed.

1 Introduction

With the beginning of RHIC operation heavy-ion physics entered a new regime, where pQCD phenomena can be fully explored. High-energy partons materializing into hadronic jets can be used as sensitive probes of the early stage of heavy ion collisions. Measurements carried out during the first two years of RHIC operation at $\sqrt{s_{NN}}=130$ and 200 GeV exhibit many surprising features. The high- p_{\perp} particle yield was found to be strongly suppressed in $Au+Au$ central collisions [1, 2], and the particle distribution in azimuthal space reveals large asymmetries attributed to sizable elliptic flow [3]. Furthermore, the azimuthal anisotropy in the region of $p_{\perp}>2.5-3$ GeV/ c , where the contribution from hydrodynamics is expected to be negligible, is found to be significant and p_{\perp} independent [4]. Another unique feature, found in RHIC data, is the observation of back-to-back jet correlation disappearance in central $Au+Au$ collisions [5]. Although tremendous progress in the understanding of these phenomena has been made, an unambiguous picture merging all observables in a consistent way still has to be developed.

The QCD medium effect on high- p_{\perp} particle production in heavy ion collisions is quantified with the *nuclear modification factor* $R_{AA}(p_{\perp})$ given by the ratio of the measured AA invariant yields to the NN collision scaled $p+p$ invariant yields (eq. (1) in [2]). With no nuclear modification of particle yield, $R_{AA}(p_{\perp}) = 1$. The large decrease of $R_{AA}(p_{\perp})$ observed in central $Au+Au$ collisions is commonly attributed to the multiple interactions of highly energetic quarks with excited nuclear medium.

¹E-mail address: janrak@bnl.gov

Induced soft-gluon radiation carries off a significant fraction of each parton's energy, which leads to the depletion of the high- p_{\perp} particle yield [6].

It is expected that the same mechanism of parton energy loss in the nuclear medium should also generate azimuthal anisotropies observed in the high- p_{\perp} region. However, as it was first pointed out by E.Shuryak [7] and B. Muller [8], the influence of the nuclear medium on parton trajectory, although sufficient for excessive yield suppression, is not capable to generate azimuthal anisotropies larger than 10%.

It has been suggested that the partonic “collective” hadronization might amplify the hadronic flow to the values of v_2 , as seen in experiment, if one assumes some sort of partonic coalescence [9, 10, 11]. The v_2 values of identified π^{\pm} , K^{\pm} and $p\bar{p}$ [12], and K_S^0 , $\Lambda\bar{\Lambda}$ [13] scaled by its quark content are apparently suggesting some kind of partonic collectivity. However, more data, especially identified particles at high- p_{\perp} , are needed.

Relatively good quantitative description of the high- p_{\perp} $v_2(p_{\perp})$ data was achieved in the model [14, 15] based on extension of the original “Color Glass Condensate” (*CGC*) model [16, 17]. The mono-jet (one gluon) radiation in classical *CGC* has been extended by including two-gluon production amplitude. This two-gluon radiation term generates two-particle azimuthal correlations, which are evidently strong enough to account for the measured strength of $v_2(p_{\perp})$. The elliptic flow in this model does not respect the reaction plane, and the azimuthal anisotropy is solely of the two-particle correlations nature. However, the absence of the correlation between spatial distribution of particle emission and the orientation of the reaction plane in this model seems to contradict some of the other observation, e.g. reaction plane dependent HBT [18]. Moreover, the recent results from $d+Au$ analysis [19] leave only small room for initial state phenomena required by *CGC* model.

In the next section we will present the analysis of the two-particle correlation function in $p+p$ collisions, where the elliptic flow correlation is not present and the jet properties can be studied in a “clean” environment.

2 Jet fragmentation in $p+p$ collisions at $\sqrt{s_{NN}}=200$ GeV

Jets are produced in the hard scattering of two partons. The schematic view of such an event in the plane perpendicular to the beam axis is shown on Fig. 1. Two scattered partons propagate back-to-back from the collision point and fragment into the jet-like spray of final state particles (only one fragment of each parton is shown). These particles have a transverse momentum \vec{j}_{\perp} with respect to the partonic transverse momentum. The magnitude of \vec{j}_{\perp} has been observed to be p_{\perp} independent (see [20]).

In the case of collinear partonic collisions the two emerging partons would have the same magnitude of transverse momenta pointing to the opposite directions. However, the partons are carrying initial intrinsic momenta \vec{k}_{\perp} before the collision happens. This affects the outgoing direction and magnitude of partonic p_{\perp} . It results in a momentum

imbalance (the partons' p_{\perp} are not equal) and an acoplanarity (transverse momentum of one jet does not lie in the plane determined by the transverse momentum of the second jet and the beam axes). The jets are not collinear and have a net transverse momentum $\sqrt{\langle p_{\perp}^2 \rangle_{pair}} = \sqrt{2} \cdot \sqrt{\langle k_{\perp}^2 \rangle}$ of magnitude [22]. If the jet axes were known,

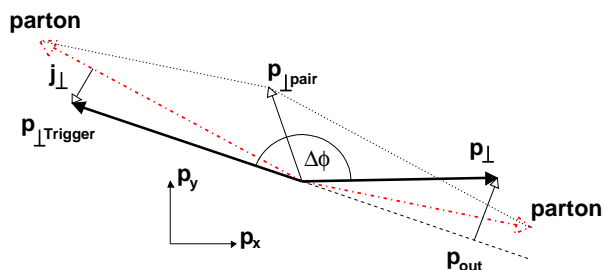


Fig. 1: The schematic view of the hard scattering event. Two back-to-back scattered partons fragment producing high- p_{\perp} particles labeled as $p_{\perp Trigger}$ and p_{\perp} , j_{\perp} denotes the jet fragmentation transverse momentum and $p_{\perp pair}$ the parton pair's net transverse momentum.

then the average projection of \vec{j}_{\perp} into the plane perpendicular to the beam axes can be determined in the following way

$$\langle |j_{\perp y}| \rangle = \langle p_{\perp} \rangle \sin \langle |\phi_i - \phi_{jet}| \rangle \quad (1)$$

where $\langle p_{\perp} \rangle$ is the average p_{\perp} of the particles produced in the fragmentation process. Here ϕ_{jet} and ϕ_i are azimuthal angles of the parton and i -th fragment respectively. However, we can only measure the relative angular dispersion between two jet fragments i and j which is $\sigma_N \equiv \sqrt{\langle (\phi_i - \phi_j)^2 \rangle} = \sqrt{2} \sqrt{\langle (\phi_i - \phi_{jet})^2 \rangle} = \sqrt{\pi} \cdot \langle |\phi_i - \phi_{jet}| \rangle$. The final formula for $\langle |j_{\perp y}| \rangle$ is

$$\langle |j_{\perp y}| \rangle = \langle p_{\perp} \rangle \cdot \sin \frac{\sigma_N}{\sqrt{\pi}} \quad (2)$$

In order to extract $\sqrt{\langle k_{\perp}^2 \rangle}$ from measured width of away side correlation peak, σ_F , we used the equation for the average transverse momentum $\langle |p_{out}| \rangle$ out of the plane defined by $\vec{p}_{Trigger}$ and the beam axis (see [20]).

$$\langle |p_{out}| \rangle^2 = \langle |j_{\perp y}| \rangle^2 + x_E^2 \langle |j_{\perp y}| \rangle^2 + 2 \langle |k_{\perp y}| \rangle^2 \quad (3)$$

where

$$x_E \equiv - \frac{\vec{p}_{\perp} \cdot \vec{p}_{\perp Trigger}}{|\vec{p}_{\perp Trigger}|^2} \quad (4)$$

with \vec{p}_\perp being the momentum of the particles produced in the opposite direction to the $\vec{p}_{\perp Trigger}$. For the case where the magnitudes of $\vec{p}_{\perp Trigger}$ and \vec{p}_\perp are similar, then

$$x_E \approx -\cos(\langle|\Delta\phi|\rangle) = -\cos\left(\sqrt{\frac{2}{\pi}}\sigma_F\right) \quad (5)$$

The magnitude of $\langle|p_{out}|\rangle$ is expressed as

$$\langle|p_{out}|\rangle = \langle p_\perp \rangle \sin(\langle|\Delta\phi|\rangle) = \langle p_\perp \rangle \sin\left(\sqrt{\frac{2}{\pi}}\sigma_F\right) \quad (6)$$

From (3) and using (2) one can derive the relation

$$\langle|k_{\perp y}|\rangle = \langle p_\perp \rangle \cos\frac{\sigma_N}{\sqrt{\pi}} \sqrt{\frac{1}{2} \tan^2\left(\sqrt{\frac{2}{\pi}}\sigma_F\right) - \tan^2\left(\sqrt{\frac{1}{\pi}}\sigma_N\right)} \quad (7)$$

In the limit of small angles, $\sigma_N \rightarrow 0$, $\sigma_F \rightarrow 0$ and equations (2) and (7) simplify to

$$\begin{aligned} \sqrt{\langle j_\perp^2 \rangle} &= \sqrt{\pi} \cdot \langle|j_{\perp y}|\rangle \approx \langle p_\perp \rangle \cdot \sigma_N \\ \sqrt{\langle k_\perp^2 \rangle} &= \sqrt{\pi} \cdot \langle|k_{\perp y}|\rangle \approx \langle p_\perp \rangle \cdot \sqrt{\sigma_F^2 - \sigma_N^2} \end{aligned} \quad (8)$$

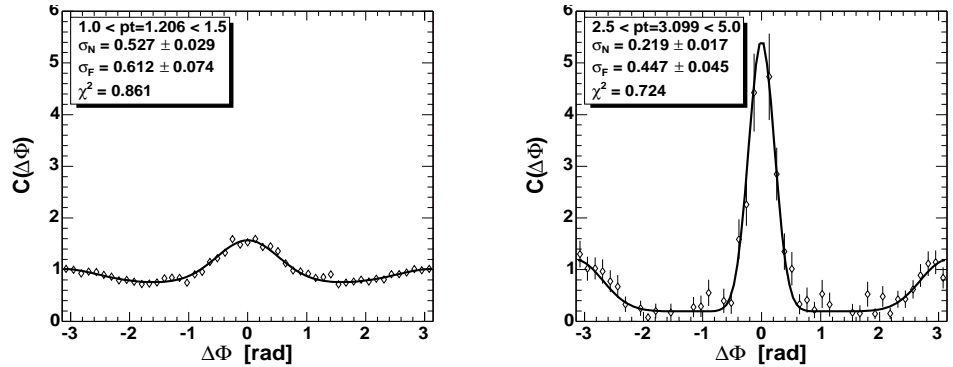


Fig. 2: Two charged hadrons area-normalized correlation function extracted from $p + p$ data for both particles in $1.0 < p_\perp < 1.5$ GeV/c (left panel) and $2.5 < p_\perp < 5.0$ GeV/c (right panel). The solid line correspond to the result of the fit (9).

An example of the two-particle correlation function (CF), defined as a ratio of “real” and “mixed” particle pairs distributions $C(\Delta\phi) = \frac{dN_{real}/d\Delta\phi}{dN_{mixed}/d\Delta\phi}$, in $p + p$ collisions is shown in Fig. 2 for $\langle p_{\perp} \rangle = 1.2$ GeV/ c (left panel) and $\langle p_{\perp} \rangle = 3.1$ GeV/ c (right panel).

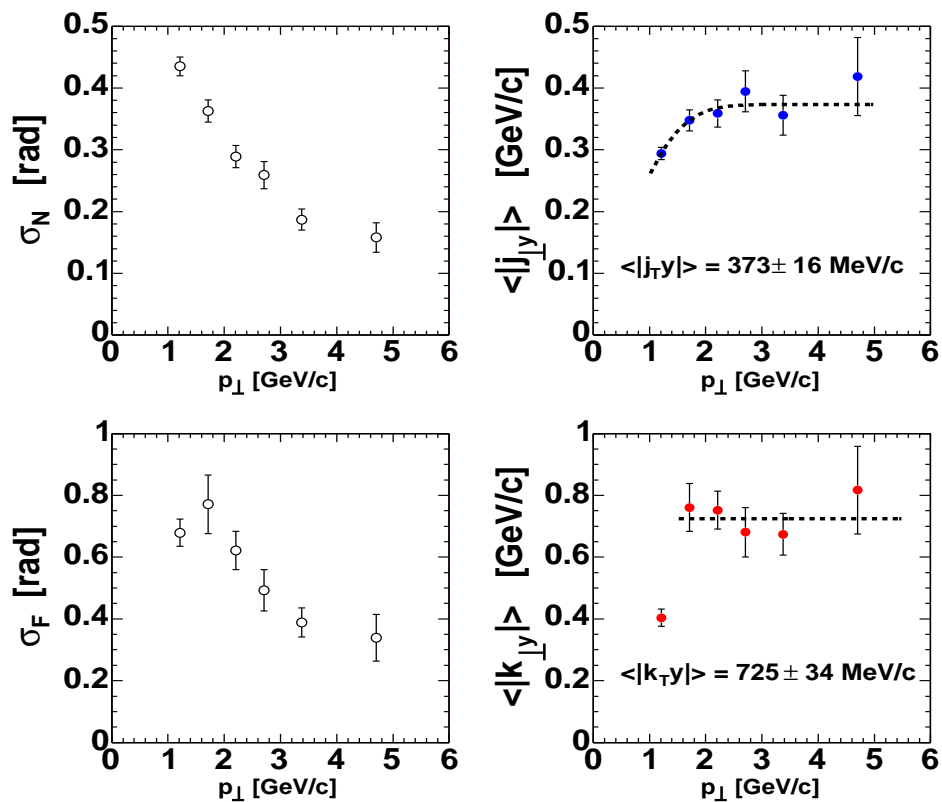


Fig. 3: Measured width of the near angle peak σ_N (upper left panel) and far angle peak σ_F (lower left panel) as a function of p_{\perp} . Extracted values of $\langle |j_{\perp y}| \rangle$ at given p_{\perp} -bins are shown on upper right panel. The dashed line corresponds to the truncated “Seagull” fit (see text). The lower right panel shows the $\langle |k_{\perp y}| \rangle$ with zeroth order polynomial fit (dashed line).

The correlation functions are area-normalized ($\int_{-\pi}^{\pi} C(\Delta\phi) = 2\pi$). A significant excess of small angle ($\Delta\phi=0$, intra-jet correlations) and large angle ($\Delta\phi = \pm\pi$, inter-jet correlations) is evident. The data were fitted by

$$Fit(C, Y_N, \sigma_N, Y_F, \sigma_F) = C + Y_N \cdot Gauss(\Delta\phi = 0, \sigma_N) + Y_F \cdot Gauss(\Delta\phi = \pm\pi, \sigma_F) \quad (9)$$

function, where C is the constant, Y_N , σ_N , Y_F and σ_F are the yields and peak widths of near and far angle peaks respectively.

The analysis of the correlation functions for various p_\perp -bins were performed. Extracted values of σ_N and σ_F are shown on Fig. 3. The angular width of the near and far angle peak is decreasing with p_\perp as expected in case of jet fragmentation. The values of $\langle |j_{\perp y}| \rangle$ and $\langle |k_{\perp y}| \rangle$ were extracted. In case of $\langle |j_{\perp y}| \rangle$ (upper right panel of Fig. 3) one can observe the reduction of $\langle |j_{\perp y}| \rangle$ extracted for lowest p_\perp -bins. This is caused by p_\perp truncation, sometimes referred as ‘‘Seagull effect’’ [23] (the j_\perp at given p_\perp cannot be larger then p_\perp itself, and thus the measured σ_N and j_\perp at $p_\perp \approx j_\perp$ is accordingly reduced.) One can easily account for such truncation and the result of the fit procedure is shown as a dashed line on upper right panel of Fig. 3.

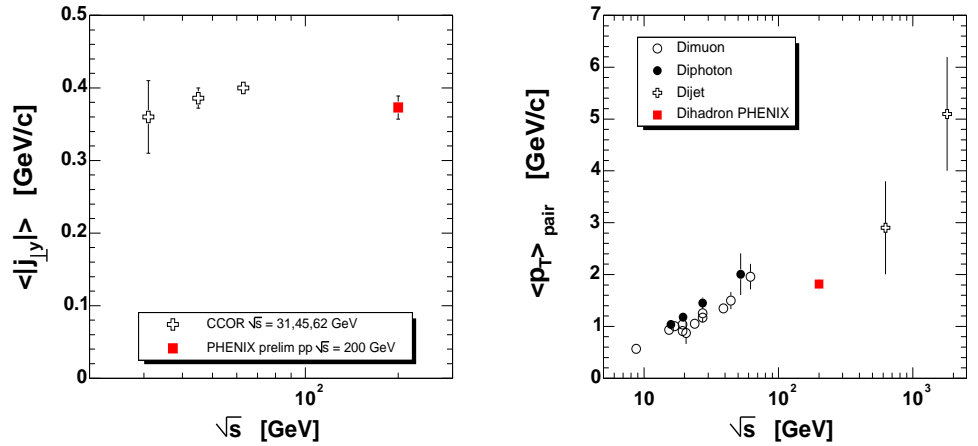


Fig. 4: The comparison of PHENIX preliminary measurement of $\langle |j_{\perp y}| \rangle$ at $\sqrt{s_{NN}} = 200$ GeV with CCOR measurement done at $\sqrt{s_{NN}} = 31, 45$ and 62 GeV (left panel). The comparison of $\sqrt{\langle p_\perp^2 \rangle_{\text{pair}}}$ extracted from PHENIX preliminary measurement on $\langle |k_{\perp y}| \rangle$ according (10) shown on right panel.

The average value is

$$\langle |j_{\perp y}| \rangle = 373 \pm 16 \text{ MeV}/c.$$

The average $\langle |k_{\perp y}| \rangle$ was extracted by fitting a constant to the data above 1.5 GeV/ c . The average value found is

$$\langle |k_{\perp y}| \rangle = 725 \pm 34 \text{ MeV}/c.$$

The comparison of $\langle |j_{\perp y}| \rangle$ with results of CCOR collaboration [20] (left panel on Fig. 4) shows a good agreement. The $\langle |k_{\perp y}| \rangle$ parameter could be compared to average RMS of the pair's momentum $\sqrt{\langle p_{\perp}^2 \rangle_{pair}}$, which has been studied on $p + \bar{p}$ Tevatron collider at Fermilab [24]. The pair's p_{\perp} is related to the individual parton $\langle |k_{\perp y}| \rangle$ by the expression

$$\sqrt{\langle p_{\perp}^2 \rangle_{pair}} = \sqrt{2} \cdot \sqrt{\langle k_{\perp}^2 \rangle} = \sqrt{2\pi} \cdot \langle |k_{\perp y}| \rangle \quad (10)$$

Extracted value of $\sqrt{\langle p_{\perp}^2 \rangle_{pair}} = 1.82 \pm 0.85$ GeV/c is in good agreement with $p + \bar{p}$ data. This value could be also compared to $\langle p_{\perp} \rangle = 1.80 \pm 0.23$ (stat) ± 0.16 (sys) GeV/c of PHENIX J/Ψ measurement [21].

3 Two-particle correlation in AA

Since the colliding heavy nuclei have a finite radius, the collision zone, except in very central collisions, has typical ‘‘almond’’ like shape with transverse dimensions of order of few fm. This geometrical azimuthal asymmetry is usually characterized by eccentricity

$$\epsilon(b) = \frac{\langle y^2 - x^2 \rangle}{\langle y^2 + x^2 \rangle} \quad (11)$$

where x and y are the coordinates of colliding nuclear constituents in transverse plane and b is the magnitude of the impact parameter. In the hydrodynamical approach [25], the original geometrical asymmetry is transformed into momentum space by means of multiple interactions between particles. The anisotropy in the momentum space is parametrized in the same way as spatial anisotropy

$$v_2(p_{\perp}, b) = \frac{\langle p_x^2 - p_y^2 \rangle}{\langle p_x^2 + p_y^2 \rangle} \quad (12)$$

where $v_2(p_{\perp}, b)$ corresponds to the second harmonic coefficient of Fourier expansion of the particles azimuthal distribution

$$\frac{dN_f}{d\phi} \propto [1 + 2v_2 \cdot \cos(2(\phi - \Psi))] \quad (13)$$

Here ϕ is the relative azimuthal angle of the particle emission with respect to the reaction plane Ψ . In the case of ‘‘pure’’ flow, when the particles' correlation is completely generated by (13), the correlation function has a form

$$\frac{dN_f}{d\Delta\phi} = \int_{-\pi}^{\pi} d\phi \frac{dN_f}{d\phi} \cdot \frac{dN_f}{d(\phi + \Delta\phi)} \propto (1 + 2v_2^2 \cdot \cos(2\Delta\phi)) \quad (14)$$

It is obvious that the azimuthal anisotropy v_2 generated by nuclear geometry cannot exceed the magnitude of eccentricity ϵ at given impact parameter.

In the “sharp sphere” approach, where the nuclear density is assumed to be constant inside and zero outside sphere of radius R , the eccentricity of a collision at impact parameter $b = |\vec{b}|$ is $\epsilon = b/2R$, and the geometrical v_2 could be as large as 1; but this approach is too idealized. When the more realistic nuclear density distribution of “Saxon-Woods” type is taken into account [26], the maximum value of ϵ barely reaches 50% (see Fig.5).

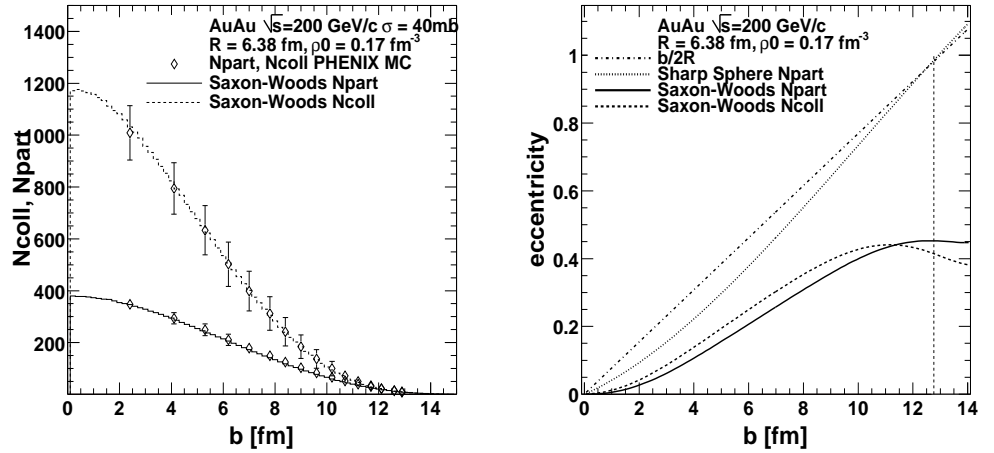


Fig. 5: Left panel: the N_{coll} and N_{part} distribution with impact parameter b computed for $Au + Au$ collisions at $\sqrt{s_{NN}}=200$ GeV. Total inelastic cross section $\sigma_{tot}=40$ mb, Au radius $R=6.38$ fm and nuclear density of 0.17 GeV/fm³ were assumed. Right panel: The eccentricity dependence on b for N_{coll} and N_{part} distributions calculated with Saxon-Woods and sharp sphere nuclear density distributions. The geometrical eccentricity $b/2R$ shown with dashed-dotted line.

However, the momentum anisotropy generated by collision geometry, irrespective of details of collision dynamics, can be only smaller. Since the anisotropy in the high- p_{\perp} region cannot be generated by hydrodynamic flow (we will ignore the initial state effects described in [14]), the expected source of observed anisotropy is the process of energy loss of high energy partons in excited nuclear medium. The upper limit on v_2 generated by jet-quenching mechanism can be computed in a similar way described in [7].

The parton born in hard scattering events inside the collision almond has to travel the distance L in the medium before it reaches the outer space. The “primordial”

azimuthal asymmetry of the medium, where the hard scattering event happened, gradually vanishes as the medium expands. Since we are searching for an upper limit on v_2 generated by jet-quenching mechanism we can neglect any dynamic and expansion of the collision zone.

The energy loss of the parton propagating through the medium could be characterized by absorption coefficient κ (dimension fm^{-3}). The probability of escaping the medium for parton born at the space point \vec{x}_0 , which propagates along the direction \vec{n} , could be expressed as

$$f(\vec{x}_0, \vec{n}) = \exp\left[-\kappa \int_0^\infty ds L_-(\vec{x}_0 + s\vec{n}) \cdot L_+(\vec{x}_0 + s\vec{n})\right]. \quad (15)$$

(see Fig. 7). Here $L_\pm(x, y) = 2[R^2 - y^2 - (x \pm b/2)^2]^{1/2}$, nuclear thicknesses along the beam axis in case of sharp sphere approach, characterizes the nuclear density at space point (x, y) and it is proportional to the probability of hard scattering [7].

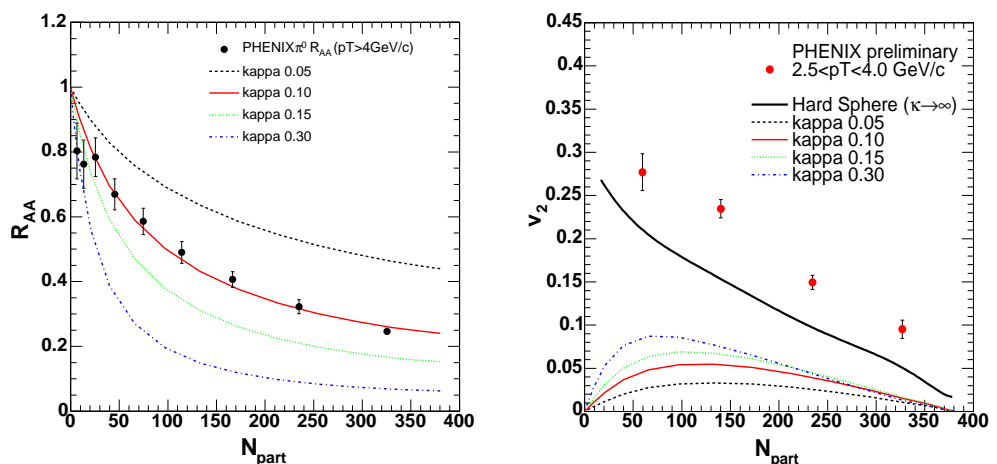


Fig. 6: Left panel: the relative absorption rates for various values of parameter κ compared to the PHENIX π^0 R_{AA} for $p_\perp > 4$ GeV/c [2]. Right panel: calculated v_2 as a function of N_{part} for the same values of parameter κ compared with the PHENIX preliminary data [3]. The solid line represents the limit from sharp sphere with $\kappa \rightarrow \infty$ (see (17)).

In more realistic Glauber model one has to replace L_-L_+ by $N_{part}(\vec{x})$ distribution, which characterizes the density of excited nuclear medium. The probability distribution of hard scattering is approximated with the product of two thickness functions

$T_A(x, y)T_B(x, y)$ (see [26]). As it was mentioned, this approach provides only an upper limit of v_2 from the jet quenching mechanism. Any more realistic scenario with a detailed calculation of partonic interactions with expanding QCD medium could lead only to reduction of the resulting v_2 .

The κ parameter is the only unknown parameter in this calculation and could be estimated from the comparison of the absorption rate dependency on collision centrality expressed in terms of N_{part} (see Fig. 6). Adjusting the absorption coefficient κ comparing to PHENIX π^0 R_{AA} for $p_\perp > 4$ GeV/ c , we found the $\kappa=0.1$ fm $^{-3}$ provides the best agreement with the data. But the maximum v_2 in this case is 6%. For less realistic values of κ the maximum value of v_2 reaches 10%. However, the values of $v_2(p_\perp)$ measured by the PHENIX collaboration using two-particle correlation techniques exceeds this maximum “jet-quenching” $v_2(p_\perp)$ by a factor of 3.

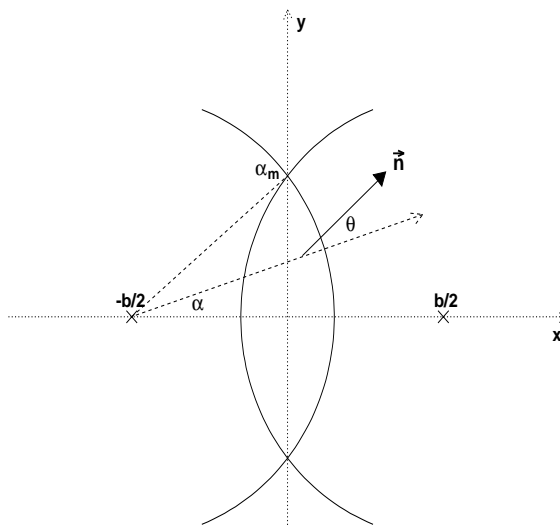


Fig. 7: The schematic view of particle production in nuclear collisions. Particle produced inside the overlap region propagates in the direction \vec{n} .

The solid line on the right panel of Fig. 6 represents an idealized limit in sharp sphere approach, when $\kappa \rightarrow \infty$, and only radiation emitted from the surface is not absorbed [27]. The escape probability P_{esc} is in the $\sigma \rightarrow \infty$ limit

$$P_{esc} = \int_0^\infty dh \exp(-\rho\sigma h / \cos\theta) \propto \cos\theta|_{\sigma \rightarrow \infty}. \quad (16)$$

where ρ stands for nuclear density, σ for absorption cross section and the product $\rho\sigma$

has similar meaning as κ parameter. The v_2 can be obtained from integration

$$v_2 = \langle \cos(2\phi) \rangle = \int d\phi P_{\text{esc}} \cdot \cos(2\phi) = \int_{-\alpha_m}^{\alpha_m} d\alpha \int_{-\pi/2}^{\pi/2} d\theta \cos\theta \frac{\cos 2(\theta + \alpha)}{2 \cdot 2\alpha} = \frac{\sin 2\alpha_m}{6\alpha_m} \quad (17)$$

where $\alpha_m = \sqrt{R^2 - (b/2)^2}$.

As one can see on Fig. 6, even the unphysical model of black body radiation providing the upper “geometrical” limit on v_2 , still does not generate enough azimuthal anisotropy as observed in data. It is evident, that in order to explain measured azimuthal anisotropies, some new underlying mechanism, other than just the “jet-quenching”, has to be invoked.

4 Summary

We have presented the detailed shape analysis of the two-hadron correlation function in $p + p$ collisions at $\sqrt{s_{NN}}=200$ GeV. The average jet-transverse momentum $\langle |j_{\perp y}| \rangle = 373 \pm 16$ MeV/c was measured. The average partons transverse momentum $\langle |k_{\perp y}| \rangle$ was extracted by fitting the constant to the data above 1.5 GeV/c, and the average value of $\langle |k_{\perp y}| \rangle = 725 \pm 34$ MeV/c was found. The comparison of $\langle |j_{\perp y}| \rangle$ with measurement done by CCOR experiment [20] shows good agreement and no significant trend with increasing $\sqrt{s_{NN}}$. The value of $\langle |k_{\perp y}| \rangle$ was compared to the values extracted from data take at Tevatron collider, and no significant deviation from the overall trend was found. The indirect measure of partonic primordial transverse momentum is the average p_{\perp} of J/Ψ mesons. Such a measurement has been done by PHENIX collaboration as well, and the value of $\langle p_{\perp} \rangle = 1.80 \pm 0.23$ (stat) ± 0.16 (sys) GeV/c has been found to be in good agreement with the $\sqrt{\langle p_{\perp}^2 \rangle}_{\text{pair}} = 1.82 \pm 0.09$ GeV/c (see eq. 10).

The analysis of two-particle correlation in $Au + Au$ at $\sqrt{s_{NN}}=200$ GeV is also presented. Using the simple Glauber model we have demonstrated that the elliptic flow parameter v_2 cannot be generated solely by jet-quenching mechanism. The upper limit for v_2 from jet-quenching has been found to be less than 10%. It is evident that the large values of v_2 observed by all RHIC experiments have to be generated by other mechanisms. There is at least one model, inspired by “Color Glass Condensate” [14], which suggests the two-gluon correlations as a source of large azimuthal anisotropies. However; the elliptic anisotropy, in this model, does not respect the reaction plane. This seems to be in contradiction with observed correlation between the reaction plane and spatial distribution of particle emission after freeze-out observed by STAR collaboration [18]. An interesting alternative provides the “coalescence” model, where the partonic flow is “amplified” by means of parton recombinations [28]. This scenario is very exciting since it requires some kind of partonic collectivity in the initial state of the collision, which is anticipated if the quark-gluon plasma is created.

References

- [1] K. Adcox *et al.*: *Phys. Rev. Lett.* **88** (2001) 022301;
- [2] S.S.. Adler *et al.*: nucl-ex/0304022 (submitted to *Phys. Rev. Lett.*);
- [3] K. Adcox *et al.*: *Phys. Rev. Lett.* **89** (2002) 212301; ;
N. N. Ajitanand for PHENIX: presentation at the QM 2002,(proceedings to be published in *Nucl. Phys. A.*);
- [4] C. Adler *et al.*: *Phys. Rev.* **C66** (2002) 034904;
- [5] C. Adler *et al.*: *Phys.Rev.Lett.* **90** (2003) 082302;
- [6] M. Gyulassy, P. Levai, I. Vitev: *Nucl.Phys.* **B594** (2001) 371-419;
- [7] E.V. Shuryak: *Phys.Rev* **C66** (2002) 027902;
- [8] B. Müller: nucl-th/0208038 (2002);
- [9] V. Greco, C.M. Ko, P. Levai: nucl-th/0305024, nucl-th/0301093 (2003);
- [10] Zi-wei Lin, Denes Molnar: nucl-th/0304045 (2003);
- [11] D. Molnar, S.A. Voloshin: nucl-th/0302014 (2003);
- [12] C. Adler *at al.*: nucl-ex/0305013 (2003);
- [13] J. Adams *at al.*: nucl-ex/0306007 (2003);
- [14] Y.V. Kovchegov, K.L. Tuchin: *Nucl.Phys* **A708** (2002) 413-434;
- [15] Y.V. Kovchegov, K.L. Tuchin: *Nucl.Phys* **A717** (2003) 249-267;
- [16] D. McLerran, R. Venugopalan: *Phys. Rev* **D49** (1994) 2233;
D. McLerran, hep-ph/0104285;
- [17] L.V. Gribov, E.M. Levin, M.G. Ryskin: *Phys. Rept.* **100** (1983) ;
D. Kharzeev, E. Levin, nucl-th/0108006;
- [18] S.Yu. Panitkin: *Heavy Ion Phys.* **15** (2002) 401-406;
- [19] S.S.. Adler *et al.*: nucl-ex/0306021 (submitted to *Phys. Rev. Lett.*);
- [20] A.L.S. Angelis *et al.*: *Phys. Lett.* **B97** (1980) 163;
- [21] “J/Psi yields from 200 GeV pp”; PHENIX; submitted to *Phys. Rev. Lett.*
- [22] M.D. Corcoran *et al.*: *Phys. Lett.* **B259** (1991) 209;
L. Apanasevich *et al.* *Phys. Rev.* **D59** (1999);
- [23] G.W. van Apeldoorn, R. Blokzijl, D.J. Holthuizen, B. Jongejans, J.C. Kluyver, J.M. Warmerdam-de Leeuw , W.J. Metzger, H.G. Tiecke, J.J.M. Timmermans: *Nucl.Phys* **B91** (1975) 1;
- [24] L. Apanasevich, C. Balazs, C. Bromberg, J. Huston, A. Maul, W.K. Tung, S. Kuhlmann, Joseph F. Owens, M. Begel, T. Ferbel, G. Ginther, P. Slattery, M. Zielinski: *Phys.Rev.* **D59** (1999) 074007;
- [25] J.Y. Ollitrault: *Phys.Rev* **D46** (1992) 229-245;
- [26] D. d’Enterria: nucl-ex/0302016, Feb 2003;
P. Shukla: nucl-th/0112039, Dec 2001;
- [27] S.A. Voloshin: nucl-ex/0210014 (2002);
- [28] R. J. Fries, B. Müller, C. Nonaka S. A. Bass: nucl-th/0306027 (2003);